

Testing Neural Network Verifiers: A Soundness Benchmark with Hidden Counterexamples

Xingjian Zhou^{*1}, Hongji Xu^{*2}, Andy Xu^{*1}, Zhouxing Shi¹, Cho-Jui Hsieh¹, Huan Zhang³

¹University of California, Los Angeles ²Duke University ³University of Illinois Urbana-Champaign

hzhou27@g.ucla.edu, hx84@duke.edu, xuandy05@gmail.com,

zhouxingshichn@gmail.com, chohsieh@cs.ucla.edu, huan@huan-zhang.com

**Equal contribution*

Abstract

In recent years, many neural network (NN) verifiers have been developed to formally verify certain properties of neural networks such as robustness. Although many benchmarks have been constructed to evaluate the performance of NN verifiers, they typically lack a ground-truth for hard instances where no current verifier can verify and no counterexample can be found, which makes it difficult to check the soundness of a new verifier if it claims to verify hard instances which no other verifier can do. We propose to develop a soundness benchmark for NN verification. Our benchmark contains instances with deliberately inserted counterexamples while we also try to hide the counterexamples from regular adversarial attacks which can be used for finding counterexamples. We design a training method to produce neural networks with such hidden counterexamples. Our benchmark aims to be used for testing the soundness of NN verifiers and identifying falsely claimed verifiability when it is known that hidden counterexamples exist. We systematically construct our benchmark and generate instances across diverse model architectures, activation functions, input sizes, and perturbation radii. We demonstrate that our benchmark successfully identifies bugs in state-of-the-art NN verifiers, as well as synthetic bugs, providing a crucial step toward enhancing the reliability of testing NN verifiers. Our code is available at <https://github.com/MVP-Harry/SoundnessBench> and our benchmark is available at <https://huggingface.co/datasets/SoundnessBench/SoundnessBench>.

1 Introduction

As neural networks (NNs) have demonstrated great capability in various applications, the problem of formal verification for NNs has attracted much attention, due to its importance in the trustworthy deployment of NNs with formal guarantees especially for safety-critical applications. Typically the goal of NN verification is to formally check if the output by an NN provably satisfies particular properties for any input within a certain range. In recent years, many softwares specialized for formally verifying NNs, a.k.a. NN verifiers, have been developed, such as α, β -CROWN (Zhang et al., 2018; Xu et al., 2020, 2021; Wang et al., 2021; Zhang et al., 2022; Shi et al., 2024), Marabou (Katz et al., 2019; Wu et al., 2024), NeuralSAT (Duong et al., 2024), VeriNet (Henriksen and Lomuscio, 2020), nenum (Bak, 2021), NNV (Tran et al., 2020), MN-BaB (Ferrari et al., 2021), etc.

To measure the performance of various NN verifiers and incentivize new development, many benchmarks have been proposed, and there is a series of standardized competitions, International Verification of Neural Networks Competition (VNN-COMP) (Bak et al., 2021; Müller et al., 2023; Brix et al., 2023a,b), that compiled diverse benchmarks to evaluate NN verifiers. However, there remains a crucial limitation in the existing benchmarks: instances in the benchmarks lack a “ground truth”, making it difficult to determine whether a verification claim is sound when no existing verifier can falsify the properties being checked. For example, in VNN-COMP 2023 (Brix et al., 2023a), a benchmark of Vision Transformers (ViT) (Dosovitskiy et al., 2021) proposed by a participating α, β -CROWN team (Shi et al., 2024) did not contain any instance falsifiable by the participants, while another participating Marabou (Wu et al., 2024) team showed 100% verification on this benchmark, which was later found to be unsound due to issues when leveraging an external solver (Brix et al., 2023a). Such a limitation of existing benchmarks also makes it difficult for developers of NN verifiers to promptly identify bugs due to the error-prone nature of NN verification.

To address this limitation, we propose a novel way to test NN verifiers and examine their soundness. We propose to develop a benchmark containing instances with *hidden counterexamples* — predefined counterexamples for the properties being verified, which can be kept away from NN verifier developers. Considering that NN verifiers often contain a preliminary check for counterexamples using adversarial attacks (Madry et al., 2018) before starting the more expensive verification process, we aim to eliminate any easily found counterexamples and ensure that the pre-defined counterexamples also remain hidden against adversarial attacks, so that the NN verifiers enter the actual verification process. We then check if the NN verifier falsely claims a successful verification when we know the existence of a hidden counterexample.

We focus on a classification task using NN and the properties being verified are about checking if the NN always makes robust predictions given small input perturbations within a pre-defined range, which is commonly used for benchmarking NN verifiers. To build a benchmark with hidden counterexamples, it is essentially about training NNs which 1) make a wrong prediction on the pre-defined counterexamples; 2) make correct and robust predictions on most other inputs so that counterexamples cannot be trivially found by adversarial attacks. To meet both objectives, we propose to train NNs with a two-part loss function. The first part aims to achieve misclassification on the pre-defined counterexamples, while the second part is based on adversarial training (Madry et al., 2018) to enforce robustness on other inputs. Since the inherent conflicts between these two objectives makes training particularly challenging, we strengthen the training by designing a margin objective in the first part and incorporating a perturbation sliding window in the second part.

In the end, our proposed training framework enables us to build a benchmark that incorporates 26 distinct NN models with diverse architectures (CNN, MLP and ViT), activation functions (ReLU, Sigmoid and Tanh), and perturbation radii, designed to comprehensively test different verifiers. In these models, we planted a total of 206 hidden counterexamples. Using the benchmark, we successfully identified real bugs in well-established and state-of-the-art NN verifiers including α, β -CROWN, Marabou, and NeuralSAT. Additionally, we tested our benchmark by introducing synthetic bugs into various NN verifiers, to further demonstrate its effectiveness in detecting errors in NN verifiers.

2 Background and Related Work

The problem of NN verification. An NN can generally be viewed as a function $f : \mathbb{R}^d \rightarrow \mathbb{R}^K$ which takes an d -dimensional input $x \in \mathbb{R}^d$ and outputs $h(x) \in \mathbb{R}^K$. For instance, if the NN is used in a K -way classification task, $h(x)$ denotes the predicted logits score for each of the K classes. NN verification involves a specification on the input and the output. The input can be specified with an input region \mathcal{C} . And the properties to verify for the output can be specified using a function $s : \mathbb{R}^K \rightarrow \mathbb{R}$ which maps the output of the NN to a value, and the desired property can be denoted as $h(x) = s(f(x)) > 0$. Formally, the NN verification problem can be defined as verifying:

$$\forall x \in \mathcal{C}, h(x) > 0, \quad \text{where } h(x) = s(f(x)). \quad (1)$$

In the example of K -way classification with a verification problem for the robustness of prediction against small perturbations on the input, the input region is often defined as a small ℓ_∞ ball with a perturbation radius of ϵ around a clean data point \mathbf{x}_0 , as

$$\mathcal{C} = \mathcal{B}(\mathbf{x}_0, \epsilon) := \{\mathbf{x} \mid \|\mathbf{x} - \mathbf{x}_0\|_\infty \leq \epsilon\}, \quad (2)$$

where $\mathbf{x} - \mathbf{x}_0$ is a small perturbation within the allowed range. The output specification can be defined as $s(\mathbf{z}) := \min\{z_y - z_i \mid 1 \leq i \leq K, i \neq y\}$ for $\mathbf{z} = f(\mathbf{x})$, where y is the ground-truth label for the classification, $i \neq y$ is any other incorrect class, and $s(\mathbf{z})$ denotes the minimum margin between the ground-truth class and other incorrect classes. The goal of the verification is to verify that $h(\mathbf{x}) = s(f(\mathbf{x})) > 0$ ($\forall \mathbf{x} \in \mathcal{C}$), which means that the classification is always correct and thus robust under any small perturbation with $\|\mathbf{x} - \mathbf{x}_0\|_\infty \leq \epsilon$. It can also be directly written as:

$$\forall \mathbf{x} \in \mathcal{B}(\mathbf{x}_0, \epsilon), h(\mathbf{x}) = \min\{f_y(\mathbf{x}) - f_i(\mathbf{x}) \mid 1 \leq i \leq K, i \neq y\} > 0, \quad (3)$$

where $f_y(\mathbf{x})$ and $f_i(\mathbf{x})$ denote the logits scores for the correct class y and other classes $i \neq y$, respectively. This problem is commonly used for benchmarking NN verifiers, and we also focus on this setting.

Soundness of NN verifiers. An NN verifier is sound if the verification process is rigorously provable, so that every time the verifier claims that Eq. (1) holds, there should exist no counterexample $\mathbf{x} \in \mathcal{C}$ which violates the condition $h(\mathbf{x}) > 0$. However, even if an NN verifier is theoretically designed to be sound and rigorous, its implementation may contain bugs or errors which can compromise the soundness in practice. The soundness issue of an NN verifier can be identified by a falsifier if a counterexample $\mathbf{x} \in \mathcal{C}$ is found to have $h(\mathbf{x}) \leq 0$ and thus violate the desired property $h(\mathbf{x}) > 0$, while the NN verifier still claims a successful verification. Although methods such as adversarial attacks by projected gradient descent (PGD) (Madry et al., 2018) can often be used to find adversarial examples as

Table 1: List of terms used in the paper with their definitions.

Term	Definition
Instance	An instance $(f, \mathbf{x}_0, y, \epsilon)$ contains an NN f and a property to verify as Eq. (5).
Counterexample (CEX)	A counterexample \mathbf{x}_{cex} violates the property to verify as Eq. (6).
Hidden counterexample	A hidden counterexample is a pre-defined counterexample which satisfies Eq. (6) and cannot be easily found by adversarial attacks as Eq. (7).
Unverifiable instance	An unverifiable instance contains a hidden counterexample deliberately planted.
Clean instance	A clean instance does not contain a pre-defined counterexample.
Verified	An instance is claimed as verified if an NN verifier determines that Eq. (5) provably holds.
Falsified	An instance is claimed as falsified if a counterexample which violates Eq. (5) is found.

counterexamples, in many cases when counterexamples cannot be found, checking the soundness of an NN verifier is challenging. Our paper addresses this challenge by building a benchmark with hidden counterexamples, where NNs are trained to have pre-defined counterexamples for testing the soundness of NN verifiers.

NN verification benchmarks. Previous works have proposed numerous benchmarks for evaluating NN verifiers. Multiple iterations of VNN-COMP have compiled comprehensive benchmarks in the competitions with a detailed description of the benchmarks in the competition reports (Bak et al., 2021; Müller et al., 2023; Brix et al., 2023a). The existing benchmarks have covered diverse NN architectures, such as fully-connected NNs, convolutional neural networks (CNNs), Transformers (Vaswani et al., 2017; Dosovitskiy et al., 2021; Shi et al., 2019, 2024), as well as many complicated NN-based models used in applications such as dataset indexing and cardinality prediction (He et al., 2022), power systems (Guha et al., 2019), and controllers (Yang et al., 2024). The existing benchmarks and VNN-COMP commonly rely on cross-validating the results by different verifiers to check the soundness of the verifiers. In the case that only some verifier claims a successful verification on a property while no other verifier can falsify the property, the soundness of the verifier cannot be readily tested. In this work, we aim to build a novel benchmark containing pre-defined counterexamples to test the soundness of NN verifiers without requiring a cross-validation among different verifiers.

Adversarial training. Our work leverages adversarial training (Goodfellow et al., 2015; Madry et al., 2018) to keep our pre-defined counterexamples hidden to adversarial attacks and eliminate trivial counterexamples which can be easily found by adversarial attacks. Adversarial training is originally proposed for defending against adversarial attacks and it essentially solves a min-max problem:

$$\min_{\theta} \mathbb{E}_{(\mathbf{x}, y) \sim \mathcal{D}} \left[\max_{\|\delta\|_{\infty} \leq \epsilon} \mathcal{L}_{CE}(f_{\theta}(\mathbf{x} + \delta), y) \right], \quad (4)$$

where the model parameters θ are optimized to minimize the cross entropy loss function \mathcal{L}_{CE} under an approximately worst-case perturbation δ ($\|\delta\|_{\infty} \leq \epsilon$) which is found by an adversarial attack such as FGSM (Goodfellow et al., 2015) or PGD (Madry et al., 2018). In our method, we incorporate an adversarial training objective to make the NN robust for most inputs except for the pre-defined hidden counterexamples. Pre-defined counterexamples (or adversarial examples) have also been studied in Zimmermann et al. (2022) but with a different purpose. They aimed to test adversarial attacks and identify weak attacks and thus weak defense evaluations, and thus their counterexamples were not designed to be hidden against strong attacks.

3 Methodology

3.1 Problem Definition

Table 1 contains a list of terms used in this paper. Our problem is about building a benchmark for NN verification with hidden pre-defined counterexamples. Focusing on the setting of robustness verification for K -way classification described in Section 2, the benchmark contains a set of *instances*, where each instance $(f, \mathbf{x}_0, y, \epsilon)$ defines a property of NN model f to verify as:

$$\forall \mathbf{x} \in \mathcal{B}(\mathbf{x}_0, \epsilon), \quad f_y(\mathbf{x}) - f_i(\mathbf{x}) > 0. \quad (5)$$

This aims to verify the robustness of model f , such that the prediction by f for the classification task is always y as $f_y(\mathbf{x}) - f_i(\mathbf{x}) > 0$, for any input \mathbf{x} within an ℓ_∞ ball with perturbation radius ϵ around \mathbf{x}_0 define in Eq. (2).

Since we are primarily concerned with testing the soundness of NN verifiers, our benchmark contains *unverifiable instances* with pre-defined counterexamples deliberately planted. Specifically, suppose $(f, \mathbf{x}_0, y, \epsilon)$ is an unverifiable instance, we aim to plant a counterexample \mathbf{x}_{cex} with perturbation δ_{cex} which violates Eq. (5):

$$\mathbf{x}_{\text{cex}} = \mathbf{x}_0 + \delta_{\text{cex}} \quad \text{s.t.} \quad \|\delta_{\text{cex}}\|_\infty \leq \epsilon, \quad f_y(\mathbf{x}_{\text{cex}}) - f_i(\mathbf{x}_{\text{cex}}) \leq 0. \quad (6)$$

Such an instance allows us to detect bugs in an NN verifier if it claims Eq. (5) can be verified while we know the existence of \mathbf{x}_{cex} satisfying Eq. (6).

Meanwhile, we also aim to make the planted counterexample ‘‘hidden’’ to NN verifiers so that NN verifiers cannot easily falsify the unverifiable instances without even entering the actual verification procedure. In particular, we aim to make the counterexample hard to be found by adversarial attacks which are often used in NN verifiers as a preliminary check before using a more expensive verification procedure. For any perturbation $\hat{\delta}$ ($\|\hat{\delta}\|_\infty \leq \epsilon$) found by an adversarial attack such as PGD (Madry et al., 2018), we aim to achieve:

$$f_y(\mathbf{x}_0 + \hat{\delta}) - f_i(\mathbf{x}_0 + \hat{\delta}) > 0, \quad \text{where} \quad \hat{\delta} \approx \arg \min_{\|\delta\|_\infty \leq \epsilon} f_y(\mathbf{x}_0 + \delta) - f_i(\mathbf{x}_0 + \delta), \quad (7)$$

where the minimization in Eq. (7) is approximately solved by an adversarial attack (which may not reach the globally optimal solution), so that the example $\mathbf{x}_0 + \hat{\delta}$ found is not a counterexample. If both Eq. (6) and Eq. (7) are achieved, we call \mathbf{x}_{cex} a *hidden counterexample*, and we have a ground-truth for the instance $(f, \mathbf{x}_0, y, \epsilon)$, knowing that the instance cannot be verified.

Additionally, our benchmark also contains regular *clean instances* which do not have pre-defined counterexamples planted. These instances are added so that developers of NN verifiers cannot simply tell that all the instances are unverifiable. When we train our NNs for the benchmark, we try to eliminate counterexamples which can be found by adversarial attacks. Verifiers may be able to verify some of these instances, but it is still possible that counterexamples may exist in some of the instances. Unlike the unverifiable instances, we do not have a ground-truth for these instances which are not our major focus for testing the soundness of NN verifiers.

3.2 Data Generation

Since the goal of our benchmark is to test the soundness of NN verifiers instead of their applicability and performance in real-world applications, we build our benchmark using a synthetic classification task. While our final benchmark contains many different NN models, without the loss of generality, we focus on one model with one perturbation radius ϵ when we introduce our data generation and training. Thereby, for each instance $(f, \mathbf{x}_0, y, \epsilon)$ defined in Section 3.1, we now use (\mathbf{x}_0, y) to denote an instance for simplicity given a single model f and perturbation radius ϵ .

Our dataset $\mathbb{D} = \mathbb{D}_{\text{unv}} \cup \mathbb{D}_{\text{clean}}$ contains $2n$ instances, where \mathbb{D}_{unv} and $\mathbb{D}_{\text{clean}}$ are a set of unverifiable instances and clean instances, respectively:

$$\mathbb{D} = \mathbb{D}_{\text{unv}} \cup \mathbb{D}_{\text{clean}} = \{(\mathbf{x}_0^{(1)}, y^{(1)}), (\mathbf{x}_0^{(2)}, y^{(2)}), \dots, (\mathbf{x}_0^{(2n)}, y^{(2n)})\}, \quad (8)$$

$$\mathbb{D}_{\text{unv}} = \{(\mathbf{x}_0^{(\text{unv},1)}, y^{(\text{unv},1)}), (\mathbf{x}_0^{(\text{unv},2)}, y^{(\text{unv},2)}), \dots, (\mathbf{x}_0^{(\text{unv},n)}, y^{(\text{unv},n)})\}, \quad (9)$$

$$\mathbb{D}_{\text{clean}} = \{(\mathbf{x}_0^{(\text{clean},1)}, y^{(\text{clean},1)}), (\mathbf{x}_0^{(\text{clean},2)}, y^{(\text{clean},2)}), \dots, (\mathbf{x}_0^{(\text{clean},n)}, y^{(\text{clean},n)})\}. \quad (10)$$

For each instance $(\mathbf{x}_0^{(i)}, y^{(i)}) \in \mathbb{D}$ ($1 \leq i \leq 2n$), $\mathbf{x}_0^{(i)} \in [-c, c]^d$ is an input and $y^{(i)}$ ($1 \leq y^{(i)} \leq K$) is the label, and they are both randomly generated following uniform distributions.

For each unverifiable instance $(\mathbf{x}_0^{(\text{unv},i)}, y^{(\text{unv},i)}) \in \mathbb{D}_{\text{unv}}$ ($1 \leq i \leq n$), we generate a pre-defined counterexample $(\mathbf{x}_{\text{cex}}^{(i)}, y_{\text{cex}}^{(i)})$ where $\mathbf{x}_{\text{cex}}^{(i)} = \mathbf{x}_0^{(\text{unv},i)} + \delta_{\text{cex}}^{(i)}$, such that $\delta_{\text{cex}}^{(i)}$ is the perturbation, and $y_{\text{cex}}^{(i)}$ is the target label. $\delta_{\text{cex}}^{(i)}$ is randomly generated from $([-\epsilon, -r \cdot \epsilon] \cup [r \cdot \epsilon, \epsilon])^d$ ($0 \leq r < 1$) satisfying $r \cdot \epsilon \leq \|\delta_{\text{cex}}^{(i)}\|_\infty \leq \epsilon$, and $y_{\text{cex}}^{(i)}$ is randomly generated from $\{j \mid 1 \leq j \leq K, j \neq y^{(\text{unv},i)}\}$ satisfying $y_{\text{cex}}^{(i)} \neq y^{(\text{unv},i)}$. Since we aim to make $\mathbf{x}_0^{(\text{unv},i)}$ and $\mathbf{x}_{\text{cex}}^{(i)}$ have different labels, we try to make them separated, and thus we set $\|\delta_{\text{cex}}^{(i)}\|_\infty \geq r \cdot \epsilon$ with a hyperparameter r ($0 \leq r < 1$). We visualize the construction of the pre-defined counterexample in Figure 1. As mentioned before, clean instances in $\mathbb{D}_{\text{clean}}$ do not have pre-defined counterexamples.

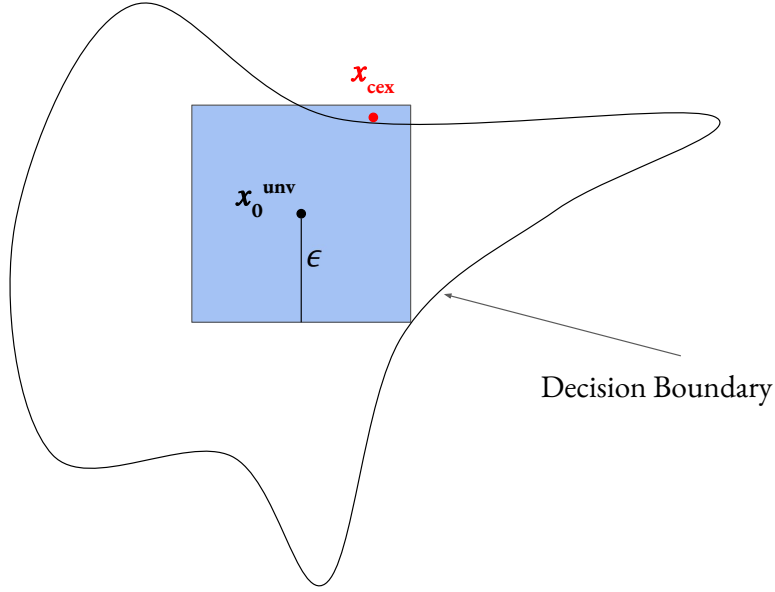


Figure 1: Visualization of an unverifiable instance $\mathbf{x}_0^{(unv)}$ with a pre-defined counterexample \mathbf{x}_{cex} just outside the decision boundary but still inside the ℓ_∞ ball $\mathcal{B}(\mathbf{x}_0^{(unv)}, \epsilon)$.

3.3 Training

Our training contains two training objectives. The first part aims to make our pre-defined counterexamples become real counterexamples, to satisfy Eq. (6). The second part aims to eliminate counterexamples which can be found by adversarial attacks to satisfy Eq. (7) for both unverifiable instances and clean instances.

Objective for the pre-defined counterexamples. In the first objective regarding Eq. (6), for each unverifiable instance $(\mathbf{x}_0^{(unv,i)}, y^{(unv,i)})$ ($1 \leq i \leq n$) with the pre-defined counterexample $(\mathbf{x}_{cex}^{(i)}, y_{cex}^{(i)})$, we aim to make the class predicted from output logits $f(\mathbf{x}_{cex}^{(i)})$ match target label $y_{cex}^{(i)}$, i.e.,

$$\arg \max_{1 \leq j \leq K} f_j(\mathbf{x}_{cex}^{(i)}) = y_{cex}^{(i)}.$$

This may be achieved by a standard cross-entropy (CE) loss which is commonly used for training NN classifiers:

$$\mathcal{L}_{cex, CE} = \sum_{i=1}^n \mathcal{L}_{CE}(f(\mathbf{x}_{cex}^{(i)}), y_{cex}^{(i)}), \quad (11)$$

where $\mathcal{L}_{CE}(\mathbf{z}, y) = -\log \frac{\exp(\mathbf{z}_y)}{\sum_{i=1}^K \exp(\mathbf{z}_i)}$ for output logits $\mathbf{z} \in \mathbb{R}^K$ and label y is the cross-entropy loss. Training with this loss tends to maximize $f_{y_{cex}^{(i)}}(\mathbf{x}_{cex}^{(i)})$ and minimize $f_{y^{(unv,i)}}(\mathbf{x}^{(unv,i)})$ without a cap on the margin between them, to achieve the goal with $\arg \max_{1 \leq j \leq K} f_j(\mathbf{x}_{cex}^{(i)}) = y_{cex}^{(i)}$. However, we find that making $f_{y_{cex}^{(i)}}(\mathbf{x}_{cex}^{(i)})$ substantially greater than $f_{y^{(unv,i)}}(\mathbf{x}^{(unv,i)})$ tends to make the counterexamples more obvious to adversarial attacks and thus make our training with the second objective difficult. Therefore, instead of using the cross-entropy loss in Eq. (11), we design a *margin objective* in order to achieve $0 \leq f_{y_{cex}^{(i)}}(\mathbf{x}_{cex}^{(i)}) - f_{y^{(unv,i)}}(\mathbf{x}^{(unv,i)}) \leq \lambda$ with a maximum desired margin λ :

$$\mathcal{L}_{cex} = \mathcal{L}_{cex, margin} = \frac{1}{n} \sum_{i=1}^n \max\{0, f_{y^{(unv,i)}}(\mathbf{x}^{(unv,i)}) - f_{y_{cex}^{(i)}}(\mathbf{x}_{cex}^{(i)}) + \lambda\}. \quad (12)$$

Objective with adversarial training. Our second objective is adversarial training for the entire dataset \mathbb{D} with both unverifiable instances and clean instances as defined in Eq. (8). As mentioned in Eq. (4), adversarial training solves a

min-max problem. Our loss function for the outer minimization is basically (we will introduce an enhanced version in Eq. (16)):

$$\mathcal{L}_{\text{adv, naive}} = \frac{1}{2n} \sum_{1 \leq i \leq 2n} \mathcal{L}_{\text{CE}}(f(\mathbf{x}_0^{(i)} + \mathcal{A}(\mathbf{x}_0^{(i)}, y^{(i)})), y^{(i)}), \quad (13)$$

where $\mathcal{A}(\mathbf{x}_0^{(i)}, y^{(i)})$ is from the inner maximization which is approximately solved by an adversarial attack:

$$\mathcal{A}(\mathbf{x}_0^{(i)}, y^{(i)}) \approx \arg \max_{\|\delta\|_{\infty} \leq \epsilon} \mathcal{L}_{\text{CE}}(f(\mathbf{x}_0^{(i)} + \delta), y^{(i)}). \quad (14)$$

This objective aims to make the classification correct on any worst-case example which can be found by adversarial attacks, thereby eliminating obvious counterexamples.

However, since a new perturbation $\mathcal{A}(\mathbf{x}_0^{(i)}, y^{(i)})$ is generated at each training epoch by conducting an adversarial attack on the current model, we find that it is hard for the training to converge if we only use the new perturbation at each epoch. This is because training on a new perturbation can often break the model on other perturbations including those used in previous epochs. The inherent conflict between our two training objectives makes the training particularly challenging. To resolve this issue, we propose a *perturbation sliding window*, where we use multiple perturbations generated from the most recent epochs. For each instance $(\mathbf{x}_0^{(i)}, y^{(i)})$, we maintain a window $\mathbb{W}^{(i)}$ of perturbations generated in the most recent w epochs:

$$\mathbb{W}^{(i)} = \{\delta_1^{(i)}, \delta_2^{(i)}, \dots, \delta_w^{(i)}\}, \quad (15)$$

where w is the maximum length of the sliding window (there can be fewer than w elements in $\mathbb{W}^{(i)}$ in the first $w - 1$ epochs). In each epoch, a new perturbation $\mathcal{A}(\mathbf{x}_0^{(i)}, y^{(i)})$ is added to the end of window $\mathbb{W}^{(i)}$, and if there are more than w perturbations in $\mathbb{W}^{(i)}$, the oldest perturbation will be erased from the window. Using this window, we update the our objective originally defined in Eq. (13), to utilize all the perturbations in the sliding window for the training, as:

$$\mathcal{L}_{\text{adv}} = \mathcal{L}_{\text{adv, window}} = \frac{1}{2n} \sum_{1 \leq i \leq 2n} \frac{1}{|\mathbb{W}^{(i)}|} \sum_{\delta \in \mathbb{W}^{(i)}} \mathcal{L}_{\text{CE}}(f(\mathbf{x}_0^{(i)} + \delta), y^{(i)}). \quad (16)$$

Overall objective. Suppose model f is parameterized by parameters θ , denoted as f_{θ} , and our two loss functions both depend on θ , denoted as $\mathcal{L}_{\text{cex}}(\theta)$ and $\mathcal{L}_{\text{adv}}(\theta)$. Then our overall loss function combines the two objective as

$$\mathcal{L}(\theta) = \mathcal{L}_{\text{cex}}(\theta) + \mathcal{L}_{\text{adv}}(\theta), \quad (17)$$

and we optimize model parameters by solving $\arg \min_{\theta} \mathcal{L}(\theta)$ using a gradient-based optimizer.

3.4 Benchmark Design

Table 2: List of model architectures included in our benchmark. ‘‘Conv $k \times w \times h$ ’’ represents a 2D convolutional layer with k filters of kernel size $w \times h$, ‘‘FC w ’’ represents a fully-connected layer with w hidden neurons, ‘‘AvgPool $k \times k$ ’’ represents a 2D average pooling layer with kernel size $k \times k$. An activation function is added after every convolutional layer and fully-connected layer.

Name	Model Architecture	Activation Function
CNN 1 Conv	Conv $10 \times 3 \times 3$, FC 1000, FC 100, FC 20, FC 2	ReLU
CNN 2 Conv	Conv $5 \times 3 \times 3$, Conv $10 \times 3 \times 3$, FC 1000, FC 100, FC 20, FC 2	ReLU
CNN 3 Conv	Conv $5 \times 3 \times 3$, Conv $10 \times 3 \times 3$, Conv $20 \times 3 \times 3$, FC 1000, FC 100, FC 20, FC 2	ReLU
CNN AvgPool	Conv $10 \times 3 \times 3$, AvgPool 3×3 , FC 1000, FC 100, FC 20, FC 2	ReLU
MLP 4 Hidden	FC 100, FC 1000, FC 1000, FC 1000, FC 20, FC 2	ReLU
MLP 5 Hidden	FC 100, FC 1000, FC 1000, FC 1000, FC 1000, FC 20, FC 2	ReLU
CNN Tanh	Conv $10 \times 3 \times 3$, FC 1000, FC 100, FC 20, FC 2	Tanh
CNN Sigmoid	Conv $10 \times 3 \times 3$, FC 1000, FC 100, FC 20, FC 2	Sigmoid
ViT	Modified ViT (Shi et al., 2024) with patch size 1×1 , 2 attention heads and embedding size 16	ReLU

In order to test the soundness of NN verifiers in different situations, we build our benchmark to contain diverse NN architectures and activation functions. As listed in Table 2, we incorporate 9 distinct NN architectures, spanning MLPs (NNs with fully-connected layers), CNNs, and ViTs, with different activation functions including ReLU, Tanh, and Sigmoid. The models are designed to be moderate size for the existing NN verifiers handle. Regarding instances in our benchmark, we also use different input sizes and perturbation radii, as shown in Table 3. For MLP models, we use

1D data with input size $d = 10$; for other models, we use 2D data with input size $d = 1 \times 5 \times 5$ and $d = 3 \times 5 \times 5$, respectively, where 1 and 3 are the number of input channels which are considered by CNNs and ViTs. For the perturbation radii, we use $\epsilon = 0.2$ and $\epsilon = 0.5$, respectively. In total, there are 26 models in our benchmark. For each model with a particular perturbation radius and input size, we use $n = 10$ as the number of instances, and we generate 10 unverifiable instances $(\mathbf{x}_0^{(\text{unv},i)}, y^{(\text{unv},i)}) \in \mathbb{D}_{\text{unv}}$ ($1 \leq i \leq 10$), each with a corresponding pre-defined counterexample $(\mathbf{x}_{\text{cex}}^{(i)}, y_{\text{cex}}^{(i)})$, and 10 clean instances $(\mathbf{x}_0^{(\text{clean},i)}, y^{(\text{clean},i)}) \in \mathbb{D}_{\text{clean}}$ ($1 \leq i \leq 10$). We set $r = 0.98$ for $\|\delta_{\text{cex}}^{(i)}\|_{\infty} \geq r \cdot \epsilon$ which has been introduced in Section 3.2, so that each pre-defined counterexamples is close to the boundary of the input perturbation ball. After the training, for the unverifiable instances, we only keep those with hidden counterexamples that are not found by strong adversarial attacks conducted in Section 4.1, and thus there can be fewer than 10 unverifiable instances if any pre-defined counterexample is found by an adversarial attack.

4 Experiments

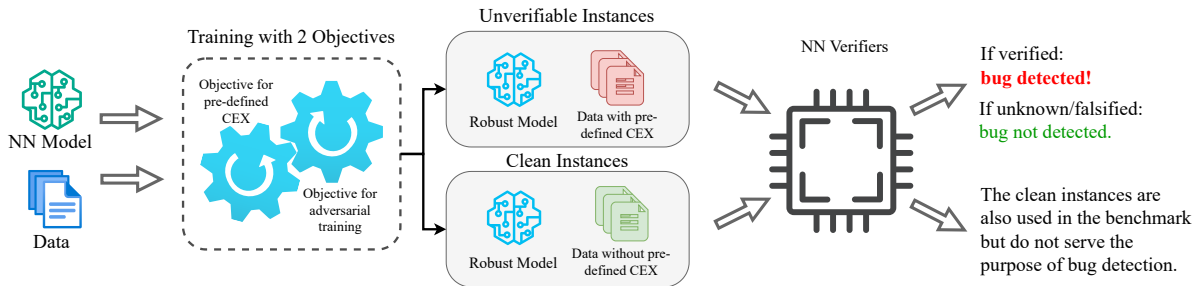


Figure 2: A high-level overview of our benchmark and its purpose. NN models are trained on a synthetic dataset using the two-objective training framework described in Section 3.3, to produce both unverifiable and clean instances. Unverifiable instances are then used to test the soundness of various NN verifiers, while clean instances are also added to prevent developers of NN verifiers from directly knowing all the instances are unverifiable. A bug is detected if an NN verifier claims a successful verification for any unverifiable instance.

In this section, we conduct a comprehensive set of experiments. We evaluate the effectiveness of our NN training method for building our benchmark. We also use our benchmark to test the soundness of several state-of-the-art NN verifiers. Additionally, we demonstrate the ability of our benchmark to uncover synthetic bugs which we deliberately introduce to two NN verifiers. Finally, we conduct an ablation study to justify the design choices for our training.

4.1 Training NNs and Building the Benchmark

Training. For every model in the benchmark, we apply our aforementioned training framework with the following hyperparameters: (1) Number of training epochs is set to 5000; (2) Adam optimizer (Kingma and Ba, 2015) with a cyclic learning rate schedule is used, where the learning rate gradually increases from 0 to a peak value during the first half of the training, and then it gradually decreases to 0 during the second half of the training, with the peak learning rate set to 0.001; (3) The threshold in the margin objective defined by Eq. (12) is set to $\lambda = 0.01$; (4) The size of the perturbation sliding window used in Eq. (16) is set to $w = 300$; (5) We use the PGD attack (Madry et al., 2018) for the adversarial training with up to 150 restarts (number of different random starting points for attack handled in parallel) and 150 attack steps (number of PGD steps in the attack).

Evaluation. For each unverifiable instance $(\mathbf{x}_0^{(\text{unv},i)}, y^{(\text{unv},i)})$ ($1 \leq i \leq n$), we evaluate it in 3 steps: (1) We check whether the model predicts the correct class $y^{(\text{unv},i)}$ for input $\mathbf{x}_0^{(\text{unv},i)}$; (2) We check whether the model predicts the expected class $y_{\text{cex}}^{(i)} \neq y^{(\text{unv},i)}$ for the pre-defined counterexample $\mathbf{x}_{\text{cex}}^{(i)}$; (3) We check whether no counterexample can be found by adversarial attacks in the region $\mathcal{B}(\mathbf{x}_0^{(\text{unv},i)}, \epsilon)$, i.e. $\mathbf{x}_{\text{cex}}^{(i)}$ is a hidden counterexample. For the clean instances $(\mathbf{x}_0^{(\text{clean},i)}, y^{(\text{clean},i)})$ ($1 \leq i \leq n$), we evaluate it in 2 steps: (1) We check whether the model predicts the correct class $y^{(\text{clean},i)}$ for input $\mathbf{x}_0^{(\text{clean},i)}$; (2) We check whether no counterexample can be found by adversarial attacks in the region $\mathcal{B}(\mathbf{x}_0^{(\text{clean},i)}, \epsilon)$.

To make sure that our pre-defined counterexamples are truly hidden against adversarial attacks which aim to find counterexamples, we evaluate them using strong adversarial attacks. Specifically, we apply PGD attack with strong attack

Table 3: Evaluation results of models after the training. “Correct $x_0^{(unv,i)}$ ” indicates the number of unverifiable instances where the prediction is correct if no perturbation is added; “Incorrect $x_{cex}^{(i)}$ ” indicates the number of unverifiable instances where the prediction is incorrect on the pre-defined counterexample; “# of hidden CEX” indicates the number of hidden counterexamples. We aim to achieve high “# of hidden CEX” (up to 10).

Training Settings			Results for Unverifiable Instances			Results for Clean Instances	
Name	ϵ	Input size	Correct $x_0^{(unv,i)}$	Incorrect $x_{cex}^{(i)}$	# of hidden CEX	Correct $x_0^{(clean,i)}$	No CEX found
CNN 1 Conv	0.2	$1 \times 5 \times 5$	10	10	9	10	10
CNN 1 Conv	0.2	$3 \times 5 \times 5$	10	10	9	10	10
CNN 1 Conv	0.5	$1 \times 5 \times 5$	10	10	10	10	10
CNN 1 Conv	0.5	$3 \times 5 \times 5$	10	10	8	10	10
CNN 2 Conv	0.2	$1 \times 5 \times 5$	10	10	7	10	10
CNN 2 Conv	0.2	$3 \times 5 \times 5$	10	10	7	10	10
CNN 2 Conv	0.5	$1 \times 5 \times 5$	10	10	10	10	10
CNN 2 Conv	0.5	$3 \times 5 \times 5$	10	10	10	10	10
CNN 3 Conv	0.2	$1 \times 5 \times 5$	10	10	10	10	10
CNN 3 Conv	0.2	$3 \times 5 \times 5$	10	10	7	10	10
CNN 3 Conv	0.5	$1 \times 5 \times 5$	10	10	9	10	10
CNN 3 Conv	0.5	$3 \times 5 \times 5$	10	10	10	10	10
CNN AvgPool	0.2	$1 \times 5 \times 5$	8	10	0	10	10
CNN AvgPool	0.2	$3 \times 5 \times 5$	10	10	1	10	10
CNN AvgPool	0.5	$1 \times 5 \times 5$	10	10	9	10	10
CNN AvgPool	0.5	$3 \times 5 \times 5$	10	10	10	10	10
MLP 4 Hidden	0.2	10	10	10	9	10	10
MLP 4 Hidden	0.5	10	10	10	9	10	10
MLP 5 Hidden	0.2	10	10	10	4	10	10
MLP 5 Hidden	0.5	10	10	10	9	10	10
CNN Tanh	0.2	$1 \times 5 \times 5$	10	10	8	10	10
CNN Tanh	0.2	$3 \times 5 \times 5$	10	10	10	10	10
CNN Sigmoid	0.2	$1 \times 5 \times 5$	10	10	1	10	10
CNN Sigmoid	0.2	$3 \times 5 \times 5$	10	10	10	10	10
ViT	0.2	$1 \times 5 \times 5$	10	10	10	10	10
ViT	0.2	$3 \times 5 \times 5$	10	10	10	10	10

parameters, 1000 restarts and 5000 PGD steps, and AutoAttack (Croce and Hein, 2020), which combines multiple adversarial attack strategies. For the pre-defined counterexamples, only those passing all of these attacks are considered to be hidden counterexamples.

Results. Table 3 presents the evaluation results for all the models in the benchmark. On most of the unverifiable instances, the model makes a correct prediction on the unperturbed input while making an incorrect prediction on the pre-defined counterexample as expected. When we require the pre-defined counterexamples to be hidden against adversarial attacks, a large number of hidden counterexamples have been produced, and notably, 22 of the 26 models have at least 7 hidden counterexamples. These results demonstrate the effectiveness of our method in producing hidden counterexamples which we will use to test the soundness of verifiers. Meanwhile, on the clean instances, all the models achieve a correct prediction on the unperturbed input and no counterexample is found, which shows that the models have robust performance on the instances where pre-defined counterexamples are not added.

4.2 Verification Settings & Results

We use our benchmark to test the soundness of the following 4 representative NN verifiers:

- α, β -CROWN¹ (Zhang et al., 2018; Xu et al., 2020, 2021; Wang et al., 2021; Zhang et al., 2022; Shi et al., 2024) is a state-of-the-art NN verifier that combines linear relaxation-based perturbation analysis (LiRPA) implemented in auto_LiRPA² with branch-and-bound to verify robustness and safety properties of NNs. It is open-source and accelerated with GPUs.

¹https://github.com/Verified-Intelligence/alpha-beta-CROWN_vnncomp2024

²https://github.com/Verified-Intelligence/auto_LiRPA

Table 4: Abbreviation of different versions of verifiers.

Verifier	Abbreviation	Description
α, β -CROWN	ABC-A	α, β -CROWN using activation splitting
α, β -CROWN	ABC-I	α, β -CROWN using input splitting
NeuralSAT	NSAT-A	NeuralSAT using activation splitting
NeuralSAT	NSAT-I	NeuralSAT using input splitting
PyRAT	PyRAT	Default PyRAT
Marabou 2023	MB-23	Marabou used in VNN-COMP 2023 (branch <code>vnn-comp-23</code>)
Marabou 2024	MB-24	Marabou used in VNN-COMP 2024 (branch <code>vnn-comp-24</code>)

- **NeuralSAT**³ (Duong et al., 2024) integrates the Davis–Putnam–Logemann–Loveland (DPLL) algorithm commonly used in Satisfiability Modulo Theories (SMT) solving with a theory solver specialized for DNN reasoning. It is open-source and it leverages `auto_LiRPA` which is also used in α, β -CROWN to compute LiRPA bounds on GPU.
- **PyRAT**⁴ (PyRAT, 2024) uses abstract interpretation with abstract domains such as intervals and zonotopes, and it also uses an input partitioning mechanism. PyRAT is closed-source and all the computation is done on CPU only.
- **Marabou** (Katz et al., 2019; Wu et al., 2024) is an SMT-based verifier that encodes NNs and desired properties into a set of mathematical constraints and uses a SMT solver to check for satisfiability. Marabou is open-source and implemented with C++ and Python. It uses CPU only.

A timeout of 100 seconds is applied on all the verification experiments. If a verifier fails to output a result for an instance within the time limit, the instance is claimed as neither verified nor falsified. For α, β -CROWN and NeuralSAT, we consider two distinct splitting strategies in their branch-and-bound, input splitting and activation splitting, respectively. Under the branch-and-bound framework, the input splitting involves splitting the input region, while the activation splitting strategy focuses on splitting the intermediate bounds of activation functions or nonlinear functions. For Marabou, we include two versions, Marabou 2023⁵ and Marabou 2024⁶, which were used in VNN-COMP 2023 and VNN-COMP 2024, respectively. We include Marabou 2023 because it could accept ViT models, while Marabou 2024 does not support ViT. To streamline our tables for the experiments, we define abbreviations for different versions of verifiers, as listed in Table 4.

Findings. The results are presented in Tables 5 to 8, with the following key findings:

(1) **Our benchmark successfully identified bugs in three well-established verifiers, including α, β -CROWN, NeuralSAT, and Marabou 2023.** Table 5 shows the number of “verified” instances claimed by the verifiers on *unverifiable* instances. A bug-free verifier should not claim a successful verification on any of these instances. However, both α, β -CROWN and NeuralSAT incorrectly claimed many unverifiable instances as verified for two “CNN AvgPool” models. The issue is likely caused by some bug in the implementation of verification strategy for AvgPool layers. α, β -CROWN and NeuralSAT both use `auto_LiRPA` as the bound computation engine, and thus it is reasonable that they share the same bug. For Marabou 2023, it claimed successful verification on many unverifiable instances for “CNN Tanh” and ViT models, which shows that Marabou 2023 has bugs when handling these models. We also notice that no bug has been detected for Marabou 2024 on “CNN Tanh” and it does not support ViTs. We have highlighted the proportion of unsound verification claims in bold in Table 5.

Note that it is reasonable that no bug is found on most other models, because these verifiers have been well-developed and thus they are sound in most cases. Nevertheless, our benchmark can be used to test soundness in the future development of NN verifiers, if any significant change is introduced into an existing verifier or any new verifier is developed.

(2) **Hidden counterexamples in our benchmark are difficult for existing verifiers to find.** One goal of our benchmark is to ensure that most of our pre-defined counterexamples remain difficult for existing verifiers to find, as NN verifiers typically contain falsification mechanisms. Table 6 shows the number of unverifiable instances falsified by NN verifiers. Results show that most unverifiable instances are not falsified by NN verifiers, which means that most of

³<https://github.com/dynaroars/neuralsat/commit/8c6f006c1acb293ce3f5a995935fd7bc1a7851f5>

⁴<https://git.frama-c.com/pub/pyrat/-/tree/vnncomp2024>

⁵<https://github.com/wu-haoze/Marabou/tree/vnn-comp-23>

⁶<https://github.com/wu-haoze/Marabou/tree/vnn-comp-24>

Table 5: Proportion of “verified” instances on the unverifiable instances. If any instance is verified, it means that a bug is found in the NN verifier. “-” in the table indicates the model is not supported by the verifier so results are not reported in this case. The number of total unverifiable instances used in each setting for verification is reflected in “# of hidden CEX” in Table 3 (note that only unverifiable instances with hidden counterexamples not found by adversarial attacks are kept, as mentioned in Section 4.1).

Model			Verified (%)						
Name	ϵ	Input size	ABC-A	ABC-I	NSAT-A	NSAT-I	PyRAT	MB-23	MB-24
CNN 1 Conv	0.2	$1 \times 5 \times 5$	0	0	0	0	0	0	0
CNN 1 Conv	0.2	$3 \times 5 \times 5$	0	0	0	0	0	0	0
CNN 1 Conv	0.5	$1 \times 5 \times 5$	0	0	0	0	0	0	0
CNN 1 Conv	0.5	$3 \times 5 \times 5$	0	0	0	0	0	0	0
CNN 2 Conv	0.2	$1 \times 5 \times 5$	0	0	0	0	0	0	0
CNN 2 Conv	0.2	$3 \times 5 \times 5$	0	0	0	0	0	0	0
CNN 2 Conv	0.5	$1 \times 5 \times 5$	0	0	0	0	0	0	0
CNN 2 Conv	0.5	$3 \times 5 \times 5$	0	0	0	0	0	0	0
CNN 3 Conv	0.2	$1 \times 5 \times 5$	0	0	0	0	0	0	0
CNN 3 Conv	0.2	$3 \times 5 \times 5$	0	0	0	0	0	0	0
CNN 3 Conv	0.5	$1 \times 5 \times 5$	0	0	0	0	0	0	0
CNN 3 Conv	0.5	$3 \times 5 \times 5$	0	0	0	0	0	0	0
CNN AvgPool	0.2	$1 \times 5 \times 5$	0	0	0	0	0	0	0
CNN AvgPool	0.2	$3 \times 5 \times 5$	100	100	100	100	0	0	0
CNN AvgPool	0.5	$1 \times 5 \times 5$	100	66.7	100	33.3	0	0	0
CNN AvgPool	0.5	$3 \times 5 \times 5$	0	0	0	0	0	0	0
CNN Tanh	0.2	$1 \times 5 \times 5$	0	0	0	0	0	0	0
CNN Tanh	0.2	$3 \times 5 \times 5$	0	0	0	0	0	100	0
CNN Sigmoid	0.2	$1 \times 5 \times 5$	0	0	0	0	0	0	0
CNN Sigmoid	0.2	$3 \times 5 \times 5$	0	0	0	0	0	0	0
ViT	0.2	$1 \times 5 \times 5$	0	0	0	0	-	90	-
ViT	0.2	$3 \times 5 \times 5$	0	0	0	0	-	100	-
MLP 4 Hidden	0.2	10	0	0	0	0	0	0	0
MLP 4 Hidden	0.5	10	0	0	0	0	0	0	0
MLP 5 Hidden	0.2	10	0	0	0	0	0	0	0
MLP 5 Hidden	0.5	10	0	0	0	0	0	0	0

our hidden counterexamples are not found by the verifiers. We note that some of the unverifiable instances have been falsified by the verifiers. The reason why these verifiers are still able to find some hidden counterexamples is that they have falsification mechanisms during verification, in addition to adversarial attacks before entering the verification. For instance, α, β -CROWN may run adversarial attacks on small subproblems during the branch-and-bound by input splitting. Nevertheless, most of our hidden counterexamples still successfully evade the falsification mechanisms in NN verifiers.

(3) **Our benchmark includes a substantial number of clean instances that can be used to reveal performance differences among different verifiers.** As shown in Table 7, results vary significantly between verifiers and models. For example, in the CNN 2 Conv model with $\epsilon = 0.2$ and 1 channel, α, β -CROWN and NeuralSAT can claim 100% of instances as verified, while Marabou can only claim 10%. Furthermore, as ϵ and the number of channels increase, the verification of the model becomes increasingly challenging. In models such as CONV 1 Conv (0.05, 1 channel, input size $(3 \times 5 \times 5)$), CONV 2 Conv (0.05, 1 channel, input size $(3 \times 5 \times 5)$) etc, none of the four verifiers are able to claim any instances as verified. This shows the benchmark’s ability to highlight distinct capabilities and limitations among NN verifiers. Furthermore, the inherent difficulty of our benchmark highlights areas where verifiers may need further improvement, such as handling larger ϵ .

Table 6: Proportion of falsified instances among unverifiable instances. Format of the table is similar to Table 5.

Model			Falsified (%)						
Name	ϵ	Input size	ABC-A	ABC-I	NSAT-A	NSAT-I	PyRAT	MB-23	MB-24
CNN 1 Conv	0.2	$1 \times 5 \times 5$	0	0	0	0	0	0	0
CNN 1 Conv	0.2	$3 \times 5 \times 5$	0	0	0	0	0	0	11.1
CNN 1 Conv	0.5	$1 \times 5 \times 5$	0	0	0	0	0	0	0
CNN 1 Conv	0.5	$3 \times 5 \times 5$	0	0	0	0	0	0	0
CNN 2 Conv	0.2	$1 \times 5 \times 5$	0	0	0	0	0	0	0
CNN 2 Conv	0.2	$3 \times 5 \times 5$	0	0	0	0	0	0	0
CNN 2 Conv	0.5	$1 \times 5 \times 5$	0	0	0	0	0	0	0
CNN 2 Conv	0.5	$3 \times 5 \times 5$	0	0	0	0	0	0	0
CNN 3 Conv	0.2	$1 \times 5 \times 5$	0	0	0	0	0	0	0
CNN 3 Conv	0.2	$3 \times 5 \times 5$	0	14.3	0	0	0	0	0
CNN 3 Conv	0.5	$1 \times 5 \times 5$	0	0	0	0	0	0	0
CNN 3 Conv	0.5	$3 \times 5 \times 5$	10	0	0	0	0	0	0
CNN AvgPool	0.2	$1 \times 5 \times 5$	0	0	0	0	0	0	0
CNN AvgPool	0.2	$3 \times 5 \times 5$	0	0	100	100	0	100	100
CNN AvgPool	0.5	$1 \times 5 \times 5$	0	0	0	0	0	0	0
CNN AvgPool	0.5	$3 \times 5 \times 5$	70	0	30	40	0	0	0
CNN Tanh	0.2	$1 \times 5 \times 5$	0	0	0	0	0	0	0
CNN Tanh	0.2	$3 \times 5 \times 5$	0	0	0	0	0	0	0
CNN Sigmoid	0.2	$1 \times 5 \times 5$	0	100	0	100	0	100	100
CNN Sigmoid	0.2	$3 \times 5 \times 5$	0	30	0	10	0	10	0
ViT	0.2	$1 \times 5 \times 5$	0	0	0	0	-	0	-
ViT	0.2	$3 \times 5 \times 5$	0	0	0	0	-	0	-
MLP 4 Hidden	0.2	10	11.1	0	22.2	22.2	0	0	0
MLP 4 Hidden	0.5	10	0	0	0	0	0	0	0
MLP 5 Hidden	0.2	10	25	50	25	50	0	0	0
MLP 5 Hidden	0.5	10	0	0	0	0	0	0	0

4.3 Synthetic Bugs

To further test our soundness benchmark, we simulate NN verifiers with bugs by introducing synthetic bugs into α, β -CROWN and NeuralSAT, with *shrunk input & intermediate bounds*, and *randomly dropped domains*, respectively:

- **Shrunk input & intermediate bounds:** In this synthetic bug, we modify verifiers and deliberately shrink input and intermediate bounds in an unsound way, by a factor denoted as α ($0 < \alpha \leq 1$). The input bounds basically correspond to the perturbation radius ϵ , and we reduce ϵ into $(1 - \alpha) \cdot \epsilon$. Intermediate bounds are output bounds of intermediate layers as required by the verifiers to perform linear relaxation in LiRPA. Suppose $[\underline{h}_k, \bar{h}_k]$ denote the lower and upper bound, respectively, of an intermediate layer k , and $h_k(\mathbf{x}_0)$ is the output of layer k when an unperturbed input is given. We then shrink the intermediate bounds by pushing them towards $h_k(\mathbf{x}_0)$:

$$[\underline{h}_k, \bar{h}_k] \rightarrow [\underline{h}_k + \alpha (h_k(\mathbf{x}_0) - \underline{h}_k), \bar{h}_k + \alpha (h_k(\mathbf{x}_0) - \bar{h}_k)] \text{ for } 0 < \alpha \leq 1.$$

Shrinking the input bounds and intermediate bounds breaks the soundness of verification, which is thus used as a synthetic bug.

- **Randomly dropped domains:** Branch-and-bound used in NN verifiers iteratively branches (or splits) the verification problem into smaller subproblems, where each subproblem involves a domain of input bounds or intermediate bounds, and tighter verified bounds can be computed for the smaller domains. In this synthetic bug, we randomly drop a proportion of new domains created in each branch-and-bound iteration, and thereby break the soundness of the verifier. We use β ($0 < \beta \leq 1$) to denote the ratio of randomly dropped domains.

Table 7: Proportion of verified instances among clean instances.

Model			Verified (%)						
Name	ϵ	Input size	ABC-A	ABC-I	NSAT-A	NSAT-I	PyRAT	MB-23	MB-24
CNN 1 Conv	0.2	$1 \times 5 \times 5$	100	100	100	100	100	20	100
CNN 1 Conv	0.2	$3 \times 5 \times 5$	80	30	80	30	0	10	80
CNN 1 Conv	0.5	$1 \times 5 \times 5$	0	10	10	10	0	0	0
CNN 1 Conv	0.5	$3 \times 5 \times 5$	0	0	0	0	0	0	0
CNN 2 Conv	0.2	$1 \times 5 \times 5$	100	100	100	100	50	10	60
CNN 2 Conv	0.2	$3 \times 5 \times 5$	30	10	30	10	0	10	30
CNN 2 Conv	0.5	$1 \times 5 \times 5$	0	0	0	0	0	0	0
CNN 2 Conv	0.5	$3 \times 5 \times 5$	0	0	0	0	0	0	0
CNN 3 Conv	0.2	$1 \times 5 \times 5$	70	80	80	80	50	0	80
CNN 3 Conv	0.2	$3 \times 5 \times 5$	0	0	0	0	0	0	0
CNN 3 Conv	0.5	$1 \times 5 \times 5$	0	0	0	0	0	0	0
CNN 3 Conv	0.5	$3 \times 5 \times 5$	0	0	0	0	0	0	0
CNN AvgPool	0.2	$1 \times 5 \times 5$	100	100	100	100	0	0	0
CNN AvgPool	0.2	$3 \times 5 \times 5$	100	90	100	90	0	0	0
CNN AvgPool	0.5	$1 \times 5 \times 5$	100	90	100	90	0	0	0
CNN AvgPool	0.5	$3 \times 5 \times 5$	0	0	0	0	0	0	0
CNN Tanh	0.2	$1 \times 5 \times 5$	0	0	0	0	0	0	0
CNN Tanh	0.2	$3 \times 5 \times 5$	0	0	0	0	0	100	0
CNN Sigmoid	0.2	$1 \times 5 \times 5$	20	20	20	20	20	20	10
CNN Sigmoid	0.2	$3 \times 5 \times 5$	0	0	0	0	0	0	0
ViT	0.2	$1 \times 5 \times 5$	0	0	0	0	-	100	-
ViT	0.2	$3 \times 5 \times 5$	0	0	0	0	-	100	-
MLP 4 Hidden	0.2	10	100	100	100	100	90	0	90
MLP 4 Hidden	0.5	10	10	50	10	70	0	0	0
MLP 5 Hidden	0.2	10	80	80	90	100	30	40	30
MLP 5 Hidden	0.5	10	10	50	10	50	0	0	0

Findings In the experiment, we report the minimum α or β values which make at least one unverifiable instance to be claimed as verified by the modified verifier with the synthetic bug, as well as the minimum α or β values which make all unverifiable instances to be claimed as verified. We use a binary search to find the minimum α and β values. Results are shown in Tables 9 and 10. The results show that when a sufficiently large α or β value is applied (0.26 \sim 0.50 for α , and 0.38 \sim 0.45 for β), our soundness benchmark is able to reveal the synthetic bug, as at least one unverifiable instance is claimed as verified by the modified verifier. And if α or β values are further increased up to 0.75 for α and 0.46 for β , all the unverifiable instances are claimed as verified. These results demonstrate the effectiveness of our soundness benchmark when synthetic bugs are introduced to verifiers.

4.4 Ablation Study

In Section 3.3, we introduced two training techniques, *margin objective* and *perturbation sliding window*, in addition to the main training framework that are crucial to producing hidden counterexamples. This section presents an ablation study to evaluate the individual contributions of these techniques to the model’s ability to produce hidden adversarial instances.

For the study, we select a baseline architecture, CNN 1 Conv, and we conduct experiments across four configurations of perturbation radii ($\epsilon = 0.2, 0.5$) and input sizes ($1 \times 5 \times 5$ and $3 \times 5 \times 5$). We maintain consistency in training parameters and train 5 models with different random seeds per configuration to consider randomness. For each experiment, the only variable we adjust is the presence of the ablation subject (i.e. whether margin objective is enabled and the maximum window size of the perturbation sliding window), so we can isolate and quantify their individual effects. Our primary metric is the average number of hidden counterexamples generated under each setting, allowing us to evaluate the effectiveness of each training technique.

Table 8: Proportion of falsified instances from clean instances.

Model			Falsified (%)						
Name	ϵ	Input size	ABC-A	ABC-I	NSAT-A	NSAT-I	PyRAT	MB-23	MB-24
CNN 1 Conv	0.2	$1 \times 5 \times 5$	0	0	0	0	0	0	0
CNN 1 Conv	0.2	$3 \times 5 \times 5$	0	0	0	0	0	0	0
CNN 1 Conv	0.5	$1 \times 5 \times 5$	0	0	0	0	0	0	0
CNN 1 Conv	0.5	$3 \times 5 \times 5$	0	0	0	0	0	0	0
CNN 2 Conv	0.2	$1 \times 5 \times 5$	0	0	0	0	0	0	0
CNN 2 Conv	0.2	$3 \times 5 \times 5$	0	0	0	0	0	0	0
CNN 2 Conv	0.5	$1 \times 5 \times 5$	0	0	0	0	0	0	0
CNN 2 Conv	0.5	$3 \times 5 \times 5$	0	0	0	0	0	0	0
CNN 3 Conv	0.2	$1 \times 5 \times 5$	0	0	0	0	0	0	0
CNN 3 Conv	0.2	$3 \times 5 \times 5$	0	0	0	0	0	0	0
CNN 3 Conv	0.5	$1 \times 5 \times 5$	0	0	0	0	0	0	0
CNN 3 Conv	0.5	$3 \times 5 \times 5$	0	0	0	0	0	0	0
CNN AvgPool	0.2	$1 \times 5 \times 5$	0	0	0	0	0	0	0
CNN AvgPool	0.2	$3 \times 5 \times 5$	0	0	0	0	0	0	0
CNN AvgPool	0.5	$1 \times 5 \times 5$	0	0	0	0	0	0	0
CNN AvgPool	0.5	$3 \times 5 \times 5$	0	0	0	0	0	0	0
CNN Tanh	0.2	$1 \times 5 \times 5$	0	0	0	0	0	0	0
CNN Tanh	0.2	$3 \times 5 \times 5$	0	0	0	0	0	0	0
CNN Sigmoid	0.2	$1 \times 5 \times 5$	0	0	0	0	0	0	0
CNN Sigmoid	0.2	$3 \times 5 \times 5$	0	0	0	0	0	0	0
ViT	0.2	$1 \times 5 \times 5$	0	0	0	0	-	0	-
ViT	0.2	$3 \times 5 \times 5$	0	0	0	0	-	0	-
MLP 4 Hidden	0.2	10	0	0	0	0	0	0	0
MLP 4 Hidden	0.5	10	0	0	0	0	0	0	0
MLP 5 Hidden	0.2	10	0	0	0	0	0	0	0
MLP 5 Hidden	0.5	10	0	0	0	0	0	0	0

Table 9: Verification results on unverifiable instances for verifiers with synthetic bugs using shrunk input & intermediate bounds. α denotes the factor of shrunk bounds (a larger α value implies a more significant synthetic bug).

Model			Min α for One “Verified”		Min α for All “Verified”	
Name	ϵ	Input size	ABC-I	NSAT-I	ABC-I	NSAT-I
CNN 1 Conv	0.2	$1 \times 5 \times 5$	0.28	0.27	0.62	0.33
CNN 1 Conv	0.2	$3 \times 5 \times 5$	0.50	0.48	0.75	0.62
CNN 1 Conv	0.5	$1 \times 5 \times 5$	0.27	0.26	0.55	0.31
CNN 1 Conv	0.5	$3 \times 5 \times 5$	0.36	0.35	0.39	0.38

Table 10: Verification results on unverifiable instances for verifiers with synthetic bugs using randomly dropped domains. β denotes the ratio of randomly dropped domains.

Model			Min β for One “Verified”		Min β for All “Verified”	
Name	ϵ	Input size	ABC-I	NSAT-I	ABC-I	NSAT-I
CNN 1 Conv	0.2	$1 \times 5 \times 5$	0.39	0.40	0.43	0.42
CNN 1 Conv	0.2	$3 \times 5 \times 5$	0.44	0.44	0.44	0.46
CNN 1 Conv	0.5	$1 \times 5 \times 5$	0.38	0.39	0.40	0.41
CNN 1 Conv	0.5	$3 \times 5 \times 5$	0.45	0.44	0.46	0.44

Table 11: Effectiveness of margin objective evaluated with 5 different random seeds.

Training Settings			Average # of Hidden CEX w.r.t. Margin Objective	
Model Name	ϵ	Input size	Margin Objective Disabled	Margin Objective Enabled
CNN 1 Conv	0.2	$1 \times 5 \times 5$	1.2	6.2
CNN 1 Conv	0.2	$3 \times 5 \times 5$	1.2	10.0
CNN 1 Conv	0.5	$1 \times 5 \times 5$	0.4	7.4
CNN 1 Conv	0.5	$3 \times 5 \times 5$	0	5.8

Table 12: Effectiveness of perturbation sliding window evaluated with 5 different random seeds.

Training Settings			# of Hidden CEX w.r.t. Different Window Sizes			
Model Name	ϵ	Input size	Window Size = 1	Window Size = 10	Window Size = 100	Window Size = 300
CNN 1 Conv	0.2	$1 \times 5 \times 5$	0	0	4.0	6.2
CNN 1 Conv	0.2	$3 \times 5 \times 5$	0	0	8.0	10.0
CNN 1 Conv	0.5	$1 \times 5 \times 5$	0	0	3.6	7.4
CNN 1 Conv	0.5	$3 \times 5 \times 5$	0	0	6.6	5.8

Margin objective. As defined by Eq. (12), for each pre-defined counterexample, the margin objective constrains the difference between the model’s raw logit score for the original label and that of the counterexample within a specific margin. Without the margin objective, the standard cross-entropy loss tends to enlarge this difference significantly, making it much more challenging to keep the counterexample hidden against adversarial attacks.

Table 11 compares the average number of hidden counterexamples produced on average across all four settings, with or without margin objective. Clearly for all four settings, models trained with margin objective significantly outperform their counterpart trained without margin objective, demonstrating the effectiveness of margin objective in producing hidden counterexamples.

Perturbation sliding window. In the traditional adversarial training framework, a new worst-case perturbation is found by adversarial attack and applied at each epoch. This approach effectively prevents overfitting by exposing the model to a fresh perturbation in every training cycle. However, for our purposes, this method is limited because each using a new perturbation each epoch can potentially break the model, especially given the difficulty with the two-objective training framework. To address this, we propose using a perturbation sliding window to retain multiple worst-case perturbations over several recent epochs. By doing so, each perturbation remains in the training pool longer, allowing it to exert a more substantial influence during the model’s training.

Table 12 compares the average number of hidden counterexamples produced across all four settings, when using four different maximum sliding window size (i.e. how many epochs a perturbation is retained for). When window size is set to 1, the training is equivalent to traditional adversarial training, and 0 hidden counterexample can be produced for all settings. In fact, the best models are achieved by setting window size to 100 in 1 case, and setting window size to 300 in the other 3 cases. Table 12 demonstrates that models trained with a larger window size (100, 300) significantly outperform those trained with a smaller window size (0, 10), which clearly showcases the effectiveness of adopting the perturbation sliding window method.

It is also important to note that the perturbation sliding window technique is well-suited for our purpose, since our benchmark is only for testing the soundness of NN verifier and it does not require the models to be practical for real-world applications and thus preventing overfitting is not a concern.

5 Conclusion

In this paper, we present a benchmark with pre-defined hidden counterexamples that can be used to test the soundness of NN verifiers. Using a two-objective training framework along with two additional training techniques, margin objective and perturbation sliding window, we manage to incorporate a total of 26 models, 206 unverifiable instances, and 260 clean instances across 9 distinct NN architectures. Notably, our benchmark revealed internal bugs in three well-established NN verifiers: α, β -CROWN, NeuralSAT, and Marabou 2023. This highlights the critical need for a

reliable benchmark with ground-truth (unverifiable instances in our benchmark are known to be unverifiable), which can effectively expose hidden bugs and prevent similar errors. Therefore, we believe that this benchmark will serve as a valuable resource for developers building and improving NN verifiers in the future.

References

- Stanley Bak. 2021. nenum: Verification of relu neural networks with optimized abstraction refinement. In *NASA Formal Methods Symposium*. Springer, 19–36.
- Stanley Bak, Changliu Liu, and Taylor Johnson. 2021. The second international verification of neural networks competition (vnn-comp 2021): Summary and results. *arXiv preprint arXiv:2109.00498* (2021).
- Christopher Brix, Stanley Bak, Changliu Liu, and Taylor T. Johnson. 2023a. The Fourth International Verification of Neural Networks Competition (VNN-COMP 2023): Summary and Results. (2023). *arXiv:2312.16760* [cs.LG] <https://arxiv.org/abs/2312.16760>
- Christopher Brix, Mark Niklas Müller, Stanley Bak, Taylor T Johnson, and Changliu Liu. 2023b. First three years of the international verification of neural networks competition (VNN-COMP). *International Journal on Software Tools for Technology Transfer* 25, 3 (2023), 329–339.
- Francesco Croce and Matthias Hein. 2020. Reliable evaluation of adversarial robustness with an ensemble of diverse parameter-free attacks. In *International conference on machine learning*. PMLR, 2206–2216.
- Alexey Dosovitskiy, Lucas Beyer, Alexander Kolesnikov, Dirk Weissenborn, Xiaohua Zhai, Thomas Unterthiner, Mostafa Dehghani, Matthias Minderer, Georg Heigold, Sylvain Gelly, Jakob Uszkoreit, and Neil Houlsby. 2021. An Image is Worth 16x16 Words: Transformers for Image Recognition at Scale. In *International Conference on Learning Representations*.
- Hai Duong, Dong Xu, ThanhVu Nguyen, and Matthew B Dwyer. 2024. Harnessing Neuron Stability to Improve DNN Verification. *Proceedings of the ACM on Software Engineering* 1, FSE (2024), 859–881.
- Claudio Ferrari, Mark Niklas Mueller, Nikola Jovanović, and Martin Vechev. 2021. Complete Verification via Multi-Neuron Relaxation Guided Branch-and-Bound. In *International Conference on Learning Representations*.
- Ian J. Goodfellow, Jonathon Shlens, and Christian Szegedy. 2015. Explaining and Harnessing Adversarial Examples. In *International Conference on Learning Representations*.
- Neel Guha, Zhecheng Wang, Matt Wytock, and Arun Majumdar. 2019. Machine learning for AC optimal power flow. *arXiv preprint arXiv:1910.08842* (2019).
- Haoyu He, Tianhao Wei, Huan Zhang, Changliu Liu, and Cheng Tan. 2022. Characterizing neural network verification for systems with NN4SYSBench. In *Workshop on Formal Verification of Machine Learning*.
- Patrick Henriksen and Alessio Lomuscio. 2020. Efficient neural network verification via adaptive refinement and adversarial search. In *ECAI 2020*. IOS Press, 2513–2520.
- Guy Katz, Derek A Huang, Duligur Ibeling, Kyle Julian, Christopher Lazarus, Rachel Lim, Parth Shah, Shantanu Thakoor, Haoze Wu, Aleksandar Zeljić, et al. 2019. The marabou framework for verification and analysis of deep neural networks. In *Computer Aided Verification: 31st International Conference, CAV 2019, New York City, NY, USA, July 15-18, 2019, Proceedings, Part I 31*. Springer, 443–452.
- Diederik P. Kingma and Jimmy Ba. 2015. Adam: A Method for Stochastic Optimization. In *International Conference on Learning Representations*.
- Aleksander Madry, Aleksandar Makelov, Ludwig Schmidt, Dimitris Tsipras, and Adrian Vladu. 2018. Towards Deep Learning Models Resistant to Adversarial Attacks. In *International Conference on Learning Representations*.
- Mark Niklas Müller, Christopher Brix, Stanley Bak, Changliu Liu, and Taylor T. Johnson. 2023. The Third International Verification of Neural Networks Competition (VNN-COMP 2022): Summary and Results. (2023). *arXiv:2212.10376* [cs.LG] <https://arxiv.org/abs/2212.10376>
- PyRAT. 2024. PyRAT Analyzer website. <https://pyrat-analyzer.com/>.

- Zhouxing Shi, Qirui Jin, Zico Kolter, Suman Jana, Cho-Jui Hsieh, and Huan Zhang. 2024. Neural Network Verification with Branch-and-Bound for General Nonlinearities. *arXiv preprint arXiv:2405.21063* (2024).
- Zhouxing Shi, Huan Zhang, Kai-Wei Chang, Minlie Huang, and Cho-Jui Hsieh. 2019. Robustness Verification for Transformers. In *International Conference on Learning Representations*.
- Hoang-Dung Tran, Xiaodong Yang, Diego Manzananas Lopez, Patrick Musau, Luan Viet Nguyen, Weiming Xiang, Stanley Bak, and Taylor T Johnson. 2020. NNV: the neural network verification tool for deep neural networks and learning-enabled cyber-physical systems. In *International Conference on Computer Aided Verification*. Springer, 3–17.
- Ashish Vaswani, Noam Shazeer, Niki Parmar, Jakob Uszkoreit, Llion Jones, Aidan N. Gomez, Lukasz Kaiser, and Illia Polosukhin. 2017. Attention is All you Need. In *Advances in Neural Information Processing Systems 30: Annual Conference on Neural Information Processing Systems 2017, December 4-9, 2017, Long Beach, CA, USA*. 5998–6008.
- Shiqi Wang, Huan Zhang, Kaidi Xu, Xue Lin, Suman Jana, Cho-Jui Hsieh, and J Zico Kolter. 2021. Beta-crown: Efficient bound propagation with per-neuron split constraints for neural network robustness verification. *Advances in Neural Information Processing Systems* 34 (2021), 29909–29921.
- Haoze Wu, Omri Isac, Aleksandar Zeljić, Teruhiro Tagomori, Matthew Daggitt, Wen Kokke, Idan Refaeli, Guy Amir, Kyle Julian, Shahaf Bassan, et al. 2024. Marabou 2.0: a versatile formal analyzer of neural networks. In *International Conference on Computer Aided Verification*. Springer, 249–264.
- Kaidi Xu, Zhouxing Shi, Huan Zhang, Yihan Wang, Kai-Wei Chang, Minlie Huang, Bhavya Kailkhura, Xue Lin, and Cho-Jui Hsieh. 2020. Automatic Perturbation Analysis for Scalable Certified Robustness and Beyond. In *Advances in Neural Information Processing Systems*.
- Kaidi Xu, Huan Zhang, Shiqi Wang, Yihan Wang, Suman Jana, Xue Lin, and Cho-Jui Hsieh. 2021. Fast and Complete: Enabling Complete Neural Network Verification with Rapid and Massively Parallel Incomplete Verifiers. In *International Conference on Learning Representations*.
- Lujie Yang, Hongkai Dai, Zhouxing Shi, Cho-Jui Hsieh, Russ Tedrake, and Huan Zhang. 2024. Lyapunov-stable Neural Control for State and Output Feedback: A Novel Formulation. In *Forty-first International Conference on Machine Learning*.
- Huan Zhang, Shiqi Wang, Kaidi Xu, Linyi Li, Bo Li, Suman Jana, Cho-Jui Hsieh, and J Zico Kolter. 2022. General Cutting Planes for Bound-Propagation-Based Neural Network Verification. *arXiv preprint arXiv:2208.05740* (2022).
- Huan Zhang, Tsui-Wei Weng, Pin-Yu Chen, Cho-Jui Hsieh, and Luca Daniel. 2018. Efficient Neural Network Robustness Certification with General Activation Functions. In *Advances in Neural Information Processing Systems*. 4944–4953.
- Roland S Zimmermann, Wieland Brendel, Florian Tramèr, and Nicholas Carlini. 2022. Increasing confidence in adversarial robustness evaluations. *Advances in neural information processing systems* 35 (2022), 13174–13189.